Astro2020 Science White Paper

MeV Emission from Pulsar Wind Nebulae: Understanding Extreme Particle Acceleration in Highly Relativistic Outflows

Thematic Areas: ☐ Planetary Systems ☐ Star and Planet Formation
☒ Formation and Evolution of Compact Objects ☐ Cosmology and Fundamental Physics
☐ Stars and Stellar Evolution ☐ Resolved Stellar Populations and their Environments
☐ Galaxy Evolution ☐ Multi-Messenger Astronomy and Astrophysics

Principal Author:
Name: Joseph D. Gelfand
Institution: NYU Abu Dhabi
Email: jg168@nyu.edu
Phone: +971 2 628 4159

Co-authors: (names and institutions)
Zorawar Wadiasingh, Goddard Space Flight Center
Oleg Kargaltsev, George Washington University
Samar Safi-Harb, University of Manitoba
Samayra Straal, NYU Abu Dhabi
Daniel Castro, Harvard-Smithsonian Center for Astrophysics
Mallory S. E. Roberts, NYU Abu Dhabi
Patrick O. Slane, Harvard-Smithsonian Center for Astrophysics
Tea Temim, Space Telescope Science Institute
Hui Li, Los Alamos National Laboratory
Silvia Zane, University College London
Harsha Blumer, West Virginia University
Abstract (optional):

1 Introduction

The Earth is constantly bombarded from outer space by energetic particles (e.g., electrons e^-, positrons e^+, protons, nuclei; (1)). Where and how these "cosmic rays" are produced is poorly understood, with various particle types and energies likely originating from different sources. Particularly mysterious is the source of high-energy $e^\pm$ produced in our Galaxy, especially those responsible for both the high fraction of e^+ in the GeV cosmic ray lepton spectrum (e.g., (2)) and the $e^\pm$ and observed excess of microwaves (e.g., (3)) and γ-rays (e.g., (4)) detected towards the Galactic center and bulge. While these particles could be evidence for exotic forms of dark matter (e.g., (5)), they might also be produced by "normal" astrophysical sources such as pulsars (e.g., (6; 7)) – the strongly magnetized, rapidly rotating neutron stars whose rotational energy powers an ultra-relativistic outflow (commonly referred to as a "pulsar wind") whose interaction with the surrounding medium creates a pulsar wind nebula (PWN; see (8) for a recent review). While the detection of TeV emission from numerous PWNe (e.g., (9; 10)) strongly suggest they contain $e^\pm$ with PeV or higher energies, how and to what energies these particles are produced is unknown, let alone their dependence on the properties of the pulsar, pulsar wind, and surrounding medium. A major reason for this uncertainty is the lack of information concerning their MeV properties, since the synchrotron emission from the highest energy $e^\pm$ peaks in this waveband. Only by combining the MeV spectrum of PWNe measured by proposed missions (e.g., AMEGO (11), LOX) with that obtained at lower (primarily radio and X-ray) and higher (TeV) photon energies by current and hopefully future (e.g., SKA, ngVLA, ATHENA, AXIS, LYNX, CTA) facilities is it possible to measure the full spectrum of $e^\pm$ in these sources. The resultant insights into the underlying acceleration mechanism would significantly impact many areas of astrophysics – from indirect searches for dark matter (as described above) to the origin of cosmic rays to the physics of relativistic outflows observed from active galactic nuclei (AGN), γ-ray bursts (GRBs), and some gravitational wave (GW) events (e.g., (12)).

2 Particle Acceleration in Pulsar Wind Nebulae

The notion that neutron stars not only create highly relativistic particles (e.g., (13)), but inject them into the surrounding medium (e.g., (14)), has been around for nearly 50 years. How they do so remains poorly understood, As shown in Figure 1, the resultant PWNe contains several possible acceleration sites – near the neutron star surface, at the edge of pulsar magnetosphere, and both "upstream" and "downstream" of the termination shock formed by the confinement of the pulsar wind by its surroundings. The physical mechanisms which accelerates particles is expected to vary between these sites:

- near the neutron star surface and light cylinder, particles are primarily accelerated by the electric potentials generated by the neutron star's rotation magnetic field,
- "upstream" of the the termination shock both magnetic reconnection and Fermi acceleration are believed to be important (see (15) for a recent review),
- while convection or turbulence "downstream" of the termination shock can result in additional magnetic reconnection within the PWN that re-accelerates previously injected particles (e.g., (16; 17; 18)).

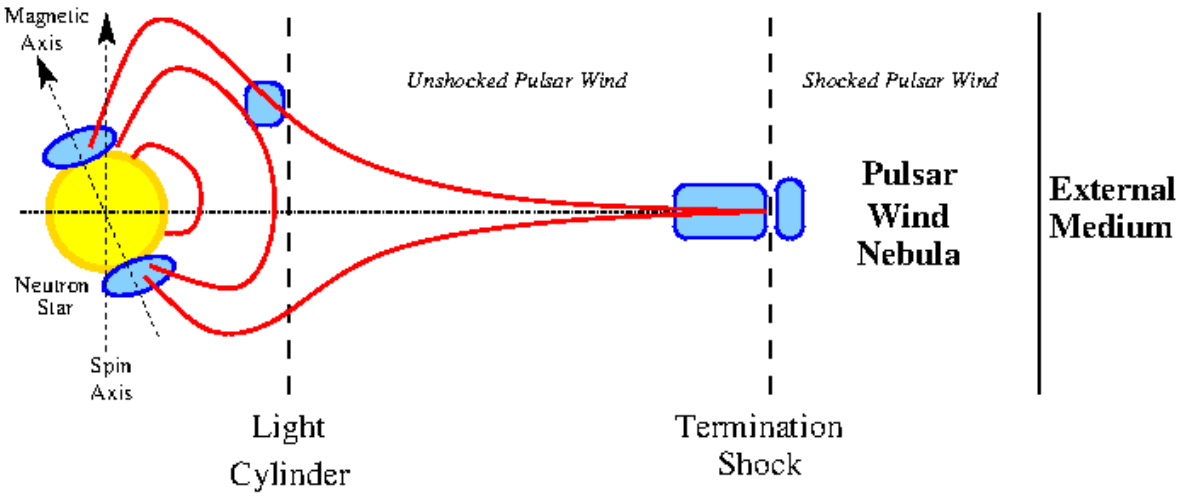

Figure 1: Schematic diagram of a PWN, with possible acceleration sites indicated by blue rectangles. The light-cylinder is located at the largest distance where particles can co-rotate with the neutron star, $r_{\rm LC} = \frac{cP}{2\pi}$ where c is the speed of light, and P is the pulsar's rotation period. Particles traveling along the field lines which extend past $r > r_{\rm LC}$ form the equatorial "pulsar wind." The confinement of this wind by the external medium creates a "termination shock," beyond which lies the shocked particles responsible for the PWN's emission.

The cumulative particle spectrum likely depends on numerous parameters, e.g., the spin-down luminosity $\dot{E}$ of the pulsar, the content and structure of the unshocked pulsar wind, the location and geometry of the termination shock, and the density of the surrounding medium. Furthermore, the evolution of the pulsar and changes in its surroundings will likely cause the relative importance of different acceleration sites, and the resultant spectrum, to vary with time. Only by measuring the properties of a PWN, for example the broadband spectral energy distribution (SED) and polarization of its radiation, is it possible to determine its particle spectrum. This information is critical for not only identifying the dominant acceleration mechanism, but understanding its dependence on the physical properties of the system and evolution in time. Particularly fruitful is the study of PWNe powered by young pulsars (§2.1) – whose large $\dot{E}$ allows one to study particle acceleration under the extremest conditions, and pulsars in binary systems (§2.2) – where the time-variable orientation and environment allows detailed study of particle acceleration at the termination shock.

2.1 Pulsar Wind Nebulae inside Supernova Remnants

When a pulsar is young, it and its PWN are embedded within the supernova remnant (SNR) produced by the progenitor explosion. Due to the high $\dot{E}$ of the central pulsar and near complete confinement of the pulsar wind by the surrounding ejecta, such PWNe can be extremely luminous. In fact, PWNe are one of few astronomical objects detected across the entire electromagnetic spectrum (e.g., (19)), with the emission at "lower" frequencies ($\nu \lesssim 10^{23}$ Hz) dominated by synchrotron radiation from $e^{\pm}$ downstream of the termination shock, while the emission at higher frequencies $\nu \gtrsim 10^{23}$ Hz is inverse Compton (IC) radiation resulting from these same $e^{\pm}$ scattering off external photon fields (e.g., the cosmic microwave background (CMB), the Galactic infrared background, and starlight) and, in rare cases, its own synchrotron emission (e.g., (20)). The emission from the highest energy particles inside the PWN does *not* appear at the highest photon energies because the IC emission from PeV (and higher) particles is

significantly attenuated by the Klein-Nishina effect (21). Studying these particles requires detecting their synchrotron emission, expected to dominate at MeV energies. Currently, there are no facilities sensitive enough to detect MeV emission from young PWNe – and haven't been since *COMPTEL*, which detected unpulsed MeV emission from two PWNe (22). As described below, proposed MeV missions like AMEGO (e.g. (11)) are capable of measuring the variable and steady MeV emission from such PWNe – critical for determining both the maximum $e^{\pm}$ energy accelerated in these sources and testing models for their production.

MeV Flares from PWNe Long thought to be a "standard" candle (19) at the highest photon energies, the detection of γ-ray flares from the Crab Nebula (23; 24) suggested an unexpected variability to the production of the highest energy particles in this source. The relatively short time scale, high photon energies, and hard spectrum of these flares is suggestive of magnetic reconnection, most likely just downstream of the termination shock (e.g., (18)). If so, the energy of these flare photons is a powerful probe of the local magnetic field in the reconnection region. The survey capability of proposed missions like AMEGO (e.g., (11)) allow such instruments to detect similar such events at MeV and GeV energies from the Crab and potentially other PWNe (e.g., Vela). Constraining the diversity in the properties (e.g., frequency, fluence, spectrum) of flares from a single PWN and across the observed population will provide vital information on how magnetic reconnection downstream of the termination shock depends on the properties of both the pulsar and pulsar wind.

Steady MeV Spectrum of PWNe Since the pulsar wind of a young PWN is confined by the surrounding SNR (Figure 3), its broadband SED reflects the time-integrated injection and evolution of the accelerated particles (see (25; 8; 26) for recent reviews). Acceleration at the different sites discussed in §2 are expected result in different temporal evolution of the maximum particle energy $E_{\rm max}$. For example, acceleration inside the magnetosphere likely has $E_{\rm max} \propto \Phi$, the electric potential at the neutron star's polar cap, resulting in $E_{\rm max} \propto \sqrt{\dot{E}}$ (e.g., (27)). Acceleration at the termination shock is very sensitive to the properties of the pulsar wind (e.g., (28)), with the maximum energy $E_{\rm max}$ determined either by saturation of the acceleration mechanism ($E_{\rm max} \propto t^0$; (29)) or confinement of particle within the termination shock (which possibly also results in $E_{\rm max} \propto \sqrt{\dot{E}}$; (30)). As shown in Figure 2, differing evolution of $E_{\rm max}$ primarily impacts the expected MeV evolution of a PWN, since the short synchrotron lifetime of these particles causes this emission to be dominated by recently injected particles, while synchrotron emission at lower energies is primarily produced by particles injected at earlier times.

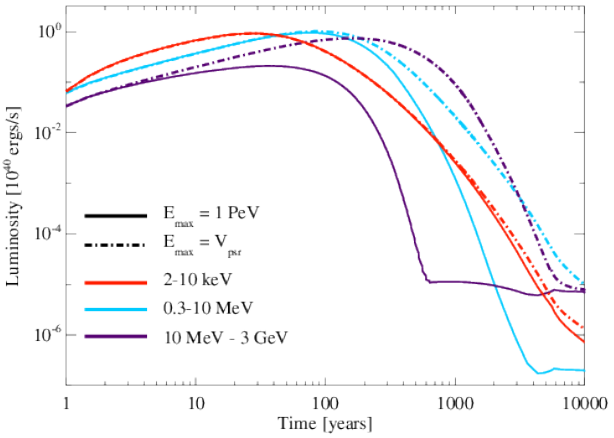

Figure 2: Expected $2-10$ keV (red), $0.3-10$ MeV (light blue), and 10 MeV $-$ 3 GeV luminosity of a PWN with constant $E_{\rm max} = 1$ PeV (solid line) and $E_{\rm max} \equiv e\Phi \propto \sqrt{\dot{E}}$ (dot-dashed line).

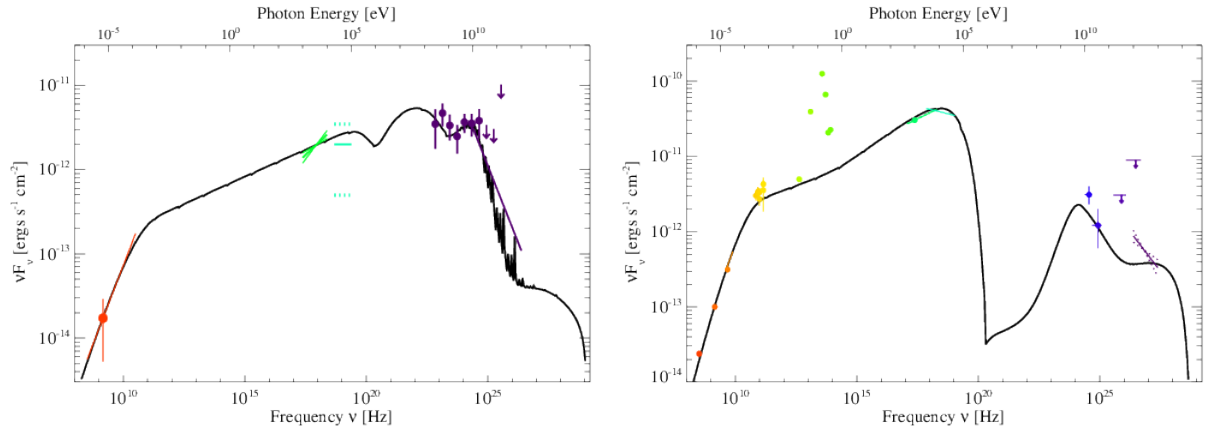

Figure 3: Observed (points) and predicted (black line) SEDs of PWNe in G11.2−0.3 (*left*) and G21.5-0.9 (*right*). The infrared red (green) points in the SED of G21.5−0.9 are significantly contaminated by hot gas surrounding this PWN, and were not used in the model fit described in the text.

Different $E_{\rm max}$ between PWNe will result in a range of expected MeV spectra and luminosities. Figure 3 shows the observed SED of two PWNe, G11.2−0.3 and G21.5−-0.9, overlaid with the theoretical SED resulting from fitting current data with a model for the PWN's evolution (assuming a constant $E_{\rm max}$; e.g., (31)). In the case of G11.2−0.3, the predicted SED has a broad "bump" between $E_\gamma \sim 1\ {\rm MeV} - 1\ {\rm GeV}$, a consequence of the synchrotron lifetime of $E = E_{\rm max} \approx 10\ {\rm PeV}$ eventually surpassing the age of this PWN. For G21.5−0.9, such modeling reproduces the observed softening in the X-ray band (e.g., (32)) by requiring a fairly low $E_{\rm max} \approx 0.3\ {\rm PeV}$. As a result, this PWN is predicted to produce little MeV emission. Only by measuring the MeV of these and other PWNe is it possible to test the values of $E_{\rm max}$ derived from such studies (e.g., (27; 33; 34; 35; 36)), critical for understanding the production of the highest energy particles in these systems.

2.2 Pulsar Wind Nebulae in Binary Systems

When a pulsar is in a binary system, its pulsar wind is confined by the wind of its stellar companion. The interaction between the pulsar and stellar winds creates an extremely heterogeneous environment, causing the conditions around the pulsar to change significantly during its orbit. Consequently, the size and geometry of the termination shock also varies during its orbit – resulting in time-dependent particle acceleration/cooling that can be studied by phase-resolved studies of the orbital modulation of its high energy emission. The pulsar's orbit also results in changing lines of sight towards the termination shock, causing the observed radiation at different orbital phases to originate from particles accelerated at different locations at the termination shock, and correspondingly beamed at different Doppler factors. As a result, phase- and energy-resolved studies then can study the acceleration particle index *spatially along the shock* (37), offering a powerful tool for studying how the particle index produced by both reconnection and diffusive shock acceleration varies with shock obliquity (38).
Additionally, the polarized keV – MeV emission pulsar binaries probes the structure of the magnetic field near the termination shock. Low energy electrons radiating at lower energies, owing to their longer cooling time, sample larger field structures near the termination shock, while higher energy particles radiating in the MeV band probe the inertial range and turbulence

structures closer to the shock front. Unlike static PWNe, these field structures (particularly in circularized systems) may be probed in a phase-dependent fashion as the system's rotation allows for a 3D reconstruction of the magnetic field near pulsar wind shocks, providing valuable information on the particle acceleration mechanisms.

Massive Star Pulsar Binaries The massive star binaries, or "γ-ray binaries" (39; 40) contain a massive O/OB-type star and a compact object with no jet or accretion, although only in B1259-63 is the pulsar nature of the compact object confirmed. About ~ 6 γ-ray binaries are known at GeV-TeV energies with two apparent in archival *CGRO-COMPTEL* data. Unlike the GeV/TeV bands, the hard X-ray to MeV does not suffer $\gamma\gamma$ opacity, nor does it suffer from photoelectric absorption in the wind of the massive star. Therefore the hard X-ray to MeV band provides a particularly "clean" look at the synchrotron component of the termination shock. Moreover, γ-ray binaries are bright with a νF_ν flux $\gtrsim 10^{-10}$ erg cm^{-2} s^{-1} enabling future polarization studies; detecting a high degree of polarization would both strongly confirmation of the synchrotron nature of the hard X-ray component and suggest the compact object is a pulsar. Additionally, characterizing the cutoff regime of the synchrotron peak and transition into IC also provides valuable insight into the acceleration mechanism, a key goal of the proposed AMEGO (11) and AdEPT (41) instruments.

Low Mass Millisecond Pulsar Binaries: The "Black Widow" and "Redback" Spiders Recent multiwavelength searches of unidentified *Fermi* sources have led to a notable increase in the number of known milli-second pulsars (MSPs), 80% of which are in binaries. This number is expected to increase prodigiously in the SKA era; MSPs in the galaxy number(42) $\sim 10^4$ and it is anticipated a large fraction will be detected/timed in the radio (43) enabling precise ephemerides for searches at higher energies. Moreover, as a group MSP binaries are more homogeneous than γ-ray binaries, permitting population studies. Two subsets are particularly interesting, the "black widows" (44) and "redbacks" (45) where the intrabinary shock either curves around the pulsar or the companion (46; 37; 47), generating shock expected to accelerate electrons to TeV energies (48). The number of redbacks already outnumbers the γ-ray binaries, with several detected(49; 50; 51; 52) by *NuSTAR* at a flux $\sim 10^{-11}$ erg cm^{-2} s^{-1}. The synchrotron component is hard PL with photon index $\Gamma \sim 1$, and exhibits no break at $30 - 80$ keV. Signals of shock emission in the *Fermi*-LAT band(53; 54; 55; 56) also suggest a peak and turnover in the MeV, in accordance with synchrotron burn-off. Besides the utility of phase-resolved spectropolarimetric studies already noted above, detection of the break in the MeV would characterize the geometry and efficiency of shock acceleration, which ultimately controlled by the $\dot{E}$ energy budget of the MSP. Such constraints would also enable more accurate estimates of irradiation feedback on the companion (47). Finally, a keV-MeV census of shock acceleration in spiders would enable more accurate estimates of their contribution to the local energetic positron excess (57).

References

[1] A. Aab, P. Abreu, M. Aglietta, and et al., *Combined fit of spectrum and composition data as measured by the Pierre Auger Observatory*, *Journal of Cosmology and Astro-Particle Physics* **2017** (Apr, 2017) 038, [arXiv:1612.07155].

[2] O. Adriani, G. C. Barbarino, G. A. Bazilevskaya, and et al., *An anomalous positron abundance in cosmic rays with energies 1.5-100GeV*, *Nature* **458** (Apr., 2009) 607–609, [arXiv:0810.4995].

[3] D. P. Finkbeiner, *Microwave Interstellar Medium Emission Observed by the Wilkinson Microwave Anisotropy Probe*, *ApJ* **614** (Oct., 2004) 186–193, [astro-ph/0311547].

[4] G. Dobler, D. P. Finkbeiner, I. Cholis, T. Slatyer, and N. Weiner, *The Fermi Haze: A Gamma-ray Counterpart to the Microwave Haze*, *ApJ* **717** (July, 2010) 825–842, [arXiv:0910.4583].

[5] G. Dobler, I. Cholis, and N. Weiner, *The Fermi Gamma-Ray Haze from Dark Matter Annihilations and Anisotropic Diffusion*, *ApJ* **741** (Nov, 2011) 25, [arXiv:1102.5095].

[6] D. Malyshev, I. Cholis, and J. Gelfand, *Pulsars versus dark matter interpretation of ATIC/PAMELA*, *Phys. Rev. D* **80** (Sep, 2009) 063005, [arXiv:0903.1310].

[7] D. Malyshev, I. Cholis, and J. D. Gelfand, *Fermi Gamma-ray Haze Via Dark Matter and Millisecond Pulsars*, *ApJ* **722** (Oct, 2010) 1939–1945, [arXiv:1002.0587].

[8] S. P. Reynolds, G. G. Pavlov, O. Kargaltsev, N. Klingler, M. Renaud, and S. Mereghetti, *Pulsar-Wind Nebulae and Magnetar Outflows: Observations at Radio, X-Ray, and Gamma-Ray Wavelengths*, *Space Science Rev.* **207** (Jul, 2017) 175–234, [arXiv:1705.08897].

[9] A. U. Abeysekara, A. Albert, R. Alfaro, and et al., *Extended gamma-ray sources around pulsars constrain the origin of the positron flux at Earth*, *Science* **358** (Nov, 2017) 911–914, [arXiv:1711.06223].

[10] H. E. S. S. Collaboration, *The H.E.S.S. Galactic plane survey*, *A&A* **612** (Apr, 2018) A1, [arXiv:1804.02432].

[11] AMEGO, *All Sky Medium Gamma-Ray Observatory*, *https://asd.gsfc.nasa.gov/amego/index.html* (2019).

[12] E. Troja, L. Piro, G. Ryan, H. van Eerten, R. Ricci, M. H. Wieringa, S. Lotti, T. Sakamoto, and S. B. Cenko, *The outflow structure of GW170817 from late-time broad-band observations*, *MNRAS* **478** (Jul, 2018) L18–L23.

[13] P. Goldreich and W. H. Julian, *Pulsar Electrodynamics*, *ApJ* **157** (Aug, 1969) 869.

[14] F. Pacini and M. Salvati, *Evolution of the Crab Nebula*, *Astrophysical Letters* **13** (Feb, 1973) 103.

[15] L. Sironi and B. Cerutti, *Particle Acceleration in Pulsar Wind Nebulae: PIC Modelling*, in *Modelling Pulsar Wind Nebulae* (D. F. Torres, ed.), vol. 446 of *Astrophysics and Space Science Library*, p. 247, Jan, 2017. arXiv:1705.10815.

[16] O. Porth, S. S. Komissarov, and R. Keppens, *Solution to the sigma problem of pulsar wind nebulae.*, *MNRAS* **431** (Apr, 2013) L48–L52, [arXiv:1212.1382].

[17] B. Olmi, L. Del Zanna, E. Amato, R. Bandiera, and N. Bucciantini, *On the magnetohydrodynamic modelling of the Crab nebula radio emission*, *MNRAS* **438** (Feb, 2014) 1518–1525, [arXiv:1310.8496].

[18] M. Lyutikov, S. Komissarov, L. Sironi, and O. Porth, *Particle acceleration in explosive relativistic reconnection events and Crab Nebula gamma-ray flares*, *Journal of Plasma Physics* **84** (Apr, 2018) 635840201, [arXiv:1804.10291].

[19] M. Meyer, D. Horns, and H. S. Zechlin, *The Crab Nebula as a standard candle in very high-energy astrophysics*, *A&A* **523** (Nov, 2010) A2, [arXiv:1008.4524].

[20] D. F. Torres, J. Martín, E. de Oña Wilhelmi, and A. Cillis, *The effects of magnetic field, age and intrinsic luminosity on Crab-like pulsar wind nebulae*, *MNRAS* **436** (Dec, 2013) 3112–3127, [arXiv:1309.5291].

[21] O. Klein and T. Nishina, *Über die Streuung von Strahlung durch freie Elektronen nach der neuen relativistischen Quantendynamik von Dirac*, *Zeitschrift fur Physik* **52** (Nov., 1929) 853–868.

[22] V. Schönfelder, K. Bennett, J. J. Blom, H. Bloemen, W. Collmar, A. Connors, R. Diehl, W. Hermsen, A. Iyudin, R. M. Kippen, J. Knödlseder, L. Kuiper, G. G. Lichti, M. McConnell, D. Morris, R. Much, U. Oberlack, J. Ryan, G. Stacy, H. Steinle, A. Strong, R. Suleiman, R. van Dijk, M. Varendorff, C. Winkler, and O. R. Williams, *The first COMPTEL source catalogue*, *Astronomy and Astrophysics Supplement Series* **143** (Apr, 2000) 145–179, [astro-ph/0002366].

[23] A. A. Abdo, M. Ackermann, M. Ajello, and et al., *Gamma-Ray Flares from the Crab Nebula*, *Science* **331** (Feb, 2011) 739, [arXiv:1011.3855].

[24] M. Tavani, A. Bulgarelli, V. Vittorini, and et al., *Discovery of Powerful Gamma-Ray Flares from the Crab Nebula*, *Science* **331** (Feb, 2011) 736, [arXiv:1101.2311].

[25] J. D. Gelfand, *Radiative Models of Pulsar Wind Nebulae*, in *Modelling Pulsar Wind Nebulae* (D. F. Torres, ed.), vol. 446, p. 161, Jan, 2017.

[26] P. Slane, *Pulsar Wind Nebulae*, p. 2159. 2017.

[27] N. Bucciantini, J. Arons, and E. Amato, *Modelling spectral evolution of pulsar wind nebulae inside supernova remnants*, *MNRAS* **410** (Jan, 2011) 381–398, [arXiv:1005.1831].

[28] L. Sironi and A. Spitkovsky, *Acceleration of Particles at the Termination Shock of a Relativistic Striped Wind*, *ApJ* **741** (Nov, 2011) 39, [arXiv:1107.0977].

[29] L. Sironi, A. Spitkovsky, and J. Arons, *The Maximum Energy of Accelerated Particles in Relativistic Collisionless Shocks*, *ApJ* **771** (Jul, 2013) 54, [arXiv:1301.5333].

[30] O. C. de Jager and A. Djannati-Ataï, *Implications of HESS Observations of Pulsar Wind Nebulae*, in *Astrophysics and Space Science Library* (W. Becker, ed.), vol. 357 of *Astrophysics and Space Science Library*, p. 451, Jan, 2009. arXiv:0803.0116.

[31] J. D. Gelfand, P. O. Slane, and W. Zhang, *A Dynamical Model for the Evolution of a Pulsar Wind Nebula Inside a Nonradiative Supernova Remnant*, *ApJ* **703** (Oct, 2009) 2051–2067, [arXiv:0904.4053].

[32] Hitomi Collaboration, *Hitomi X-ray observation of the pulsar wind nebula G21.5-0.9*, *Publications of the Astronomical Society of Japan* **70** (Jun, 2018) 38, [arXiv:1802.05068].

[33] J. D. Gelfand, P. O. Slane, and T. Temim, *The properties of the progenitor, neutron star, and pulsar wind in the supernova remnant Kes 75*, *Astronomische Nachrichten* **335** (Mar, 2014) 318–323.

[34] J. D. Gelfand, P. O. Slane, and T. Temim, *The Properties of the Progenitor Supernova, Pulsar Wind, and Neutron Star inside PWN G54.1+0.3*, *ApJ* **807** (Jul, 2015) 30, [arXiv:1508.01355].

[35] S. J. Tanaka and F. Takahara, *Study of Four Young TeV Pulsar Wind Nebulae with a Spectral Evolution Model*, *ApJ* **741** (Nov, 2011) 40, [arXiv:1108.1690].

[36] D. F. Torres, A. Cillis, J. Martín, and E. de Oña Wilhelmi, *Time-dependent modeling of TeV-detected, young pulsar wind nebulae*, *Journal of High Energy Astrophysics* **1** (May, 2014) 31–62, [arXiv:1402.5485].

[37] Z. Wadiasingh, A. K. Harding, C. Venter, M. Böttcher, and M. G. Baring, *Constraining Relativistic Bow Shock Properties in Rotation-powered Millisecond Pulsar Binaries*, *ApJ* **839** (Apr., 2017) 80, [arXiv:1703.09560].

[38] E. J. Summerlin and M. G. Baring, *Diffusive Acceleration of Particles at Oblique, Relativistic, Magnetohydrodynamic Shocks*, *ApJ* **745** (Jan., 2012) 63, [arXiv:1110.5968].

[39] G. Dubus, *Gamma-ray binaries and related systems*, *A&A Rev* **21** (Aug., 2013) 64, [arXiv:1307.7083].

[40] G. Dubus, *Gamma-ray emission from binaries in context*, *Comptes Rendus Physique* **16** (Aug., 2015) 661–673, [arXiv:1507.00935].

[41] S. D. Hunter, P. F. Bloser, G. O. Depaola, M. P. Dion, G. A. DeNolfo, A. Hanu, M. Iparraguirre, J. Legere, F. Longo, M. L. McConnell, S. F. Nowicki, J. M. Ryan, S. Son, and F. W. Stecker, *A pair production telescope for medium-energy gamma-ray polarimetry*, *Astroparticle Physics* **59** (Jul, 2014) 18–28, [arXiv:1311.2059].

[42] P. L. Gonthier, A. K. Harding, E. C. Ferrara, S. E. Frederick, V. E. Mohr, and Y.-M. Koh, *Population Syntheses of Millisecond Pulsars from the Galactic Disk and Bulge*, *ApJ* **863** (Aug., 2018) 199, [arXiv:1806.11215].

[43] E. Keane, B. Bhattacharyya, M. Kramer, B. Stappers, E. F. Keane, B. Bhattacharyya, M. Kramer, B. W. Stappers, S. D. Bates, M. Burgay, S. Chatterjee, D. J. Champion, R. P. Eatough, J. W. T. Hessels, G. Janssen, K. J. Lee, J. van Leeuwen, J. Margueron, M. Oertel, A. Possenti, S. Ransom, G. Theureau, and P. Torne, *A Cosmic Census of Radio Pulsars with the SKA*, *Advancing Astrophysics with the Square Kilometre Array (AASKA14)* (Apr., 2015) 40, [arXiv:1501.00056].

[44] W. Kluzniak, M. Ruderman, J. Shaham, and M. Tavani, *Nature and evolution of the eclipsing millisecond binary pulsar PSR1957 + 20*, *Nature* **334** (July, 1988) 225–227.

[45] M. S. E. Roberts, *New Black Widows and Redbacks in the Galactic Field*, in *American Institute of Physics Conference Series* (M. Burgay, N. D'Amico, P. Esposito, A. Pellizzoni, and A. Possenti, eds.), vol. 1357 of *American Institute of Physics Conference Series*, pp. 127–130, Aug., 2011. arXiv:1103.0819.

[46] R. W. Romani and N. Sanchez, *Intra-binary Shock Heating of Black Widow Companions*, *ApJ* **828** (Sep, 2016) 7, [arXiv:1606.03518].

[47] Z. Wadiasingh, C. Venter, A. K. Harding, M. Böttcher, and P. Kilian, *Pressure Balance and Intrabinary Shock Stability in Rotation-powered-state Redback and Transitional Millisecond Pulsar Binary Systems*, *ApJ* **869** (Dec., 2018) 120, [arXiv:1810.12958].

[48] A. K. Harding and T. K. Gaisser, *Acceleration by pulsar winds in binary systems*, *ApJ* **358** (Aug., 1990) 561–574.

[49] S. P. Tendulkar, C. Yang, H. An, V. M. Kaspi, A. M. Archibald, C. Bassa, E. Bellm, S. Bogdanov, F. A. Harrison, J. W. T. Hessels, G. H. Janssen, A. G. Lyne, A. Patruno, B. Stappers, D. Stern, J. A. Tomsick, S. E. Boggs, D. Chakrabarty, F. E. Christensen, W. W. Craig, C. A. Hailey, and W. Zhang, *NuSTAR Observations of the State Transition of Millisecond Pulsar Binary PSR J1023+0038*, *ApJ* **791** (Aug., 2014) 77, [arXiv:1406.7009].

[50] A. K. H. Kong, C. Y. Hui, J. Takata, K. L. Li, and P. H. T. Tam, *A NuSTAR Observation of the Gamma-Ray Emitting Millisecond Pulsar PSR J1723-2837*, *ApJ* **839** (Apr., 2017) 130, [arXiv:1703.10164].

[51] A. K. H. Kong, J. Takata, C. Y. Hui, J. Zhao, K. L. Li, and P. H. T. Tam, *Broad-band high-energy emissions of the redback millisecond pulsar PSR J2129-0429*, *MNRAS* **478** (Aug, 2018) 3987–3993, [arXiv:1806.01312].

[52] H. Al Noori, M. S. E. Roberts, R. A. Torres, M. A. McLaughlin, P. A. Gentile, J. W. T. Hessels, P. S. Ray, M. Kerr, and R. P. Breton, *X-Ray and Optical Studies of the Redback System PSR J2129–0429*, *ApJ* **861** (July, 2018) 89.

[53] Y. Xing and Z. Wang, *Discovery of Gamma-Ray Orbital Modulation in the Black Widow PSR J1311-3430*, *ApJL* **804** (May, 2015) L33, [arXiv:1502.04783].

[54] H. An, R. W. Romani, T. Johnson, M. Kerr, and C. J. Clark, *High-energy Variability of PSR J1311-3430*, *ApJ* **850** (Nov., 2017) 100, [arXiv:1710.06097].

[55] C. W. Ng, J. Takata, J. Strader, K. L. Li, and K. S. Cheng, *Evidence on the Orbital Modulated Gamma-Ray Emissions from the Redback Candidate 3FGL J2039.6–5618*, *ApJ* **867** (Nov., 2018) 90.

[56] H. An, R. W. Romani, and M. Kerr, *Signatures of Intra-binary Shock Emission in the Black Widow Pulsar Binary PSR J2241–5236*, *ApJL* **868** (Nov., 2018) L8, [arXiv:1810.13055].

[57] C. Venter, A. Kopp, A. K. Harding, P. L. Gonthier, and I. Büsching, *Cosmic-ray Positrons from Millisecond Pulsars*, *ApJ* **807** (July, 2015) 130, [arXiv:1506.01211].